

# Mapping Peptides Correlated with Transmission of Intrasteric Inhibition and Allosteric Activation in Human Cystathionine $\beta$ -Synthase<sup>†</sup>

Suvajit Sen, Jiong Yu, Mamoru Yamanishi, Daniel Schellhorn, and Ruma Banerjee\*

Biochemistry Department, University of Nebraska, Lincoln, Nebraska 68588-0664

Received June 2, 2005; Revised Manuscript Received August 29, 2005

**ABSTRACT:** Cystathionine  $\beta$ -synthase plays a key role in the intracellular disposal of homocysteine and is the single most common locus of mutations associated with homocystinuria. Elevated levels of homocysteine are correlated with heart disease, Alzheimer's and Parkinson's diseases, and neural tube defects. Cystathionine  $\beta$ -synthase is modular and subjected to complex regulation, but insights into the structural basis of this regulation are lacking. We have employed hydrogen exchange mass spectrometry to map peptides whose motions are correlated with transmission of intrasteric inhibition and allosteric activation. The mass spectrometric data provide an excellent correlation between kinetically and conformationally distinguishable states of the enzyme. We also demonstrate that a pathogenic regulatory domain mutant, D444N, is conformationally locked in one of two states sampled by the wild type enzyme. Our hydrogen exchange data identify surfaces that are potentially involved in the juxtaposition of the regulatory and catalytic domains and form the basis of a docked structural model for the full-length enzyme.

Equilibration between different conformational states often poses problems for crystallization of modular proteins, thus limiting access to structural information. Hydrogen exchange mass spectrometry is a powerful approach that can partially circumvent this limitation. Thus, motions that are correlated with interconversion between conformational states or with transduction of signals from sites distal to active sites can be localized (1, 2). Human cystathionine  $\beta$ -synthase is an example of a modular protein that catalyzes the condensation of homocysteine and serine to give cystathionine. This represents the first step in the transsulfuration pathway that connects the methionine cycle to cysteine production and also provides an avenue for disposal of sulfur under conditions of excess (3, 4). The structure of a truncated catalytic core (5, 6) but not of the full-length protein is available, limiting structural insights into the dynamics that underlie exertion of the complex regulation associated with this enzyme.

Cystathionine  $\beta$ -synthase is unique in being a PLP-dependent enzyme that also contains a heme b cofactor of unknown function (7). In this enzyme, a central catalytic core houses the active site and is interposed between an N-terminal heme domain and a C-terminal regulatory domain (Figure 1) (3, 4). The regulatory domain per se exerts intrasteric control over the catalytic module and its deletion results in an active form of the enzyme that displays a 4-fold higher  $k_{\text{cat}}$  but is unresponsive to the allosteric effector, S-adenosylmethionine (AdoMet)<sup>1</sup> (8, 9). The regulatory domain is also important in the oligomeric architecture of the protein, and its deletion converts the native tetrameric

( $\alpha_4$ ) enzyme to a dimeric ( $\alpha_2$ ) form. This transformation from the full-length to the truncated form lacking the regulatory domain is observed in cells treated with the cytokine, TNF $\alpha$ , or in mice challenged with the proinflammatory agent, lipopolysaccharide (10). A more modest activation of the enzyme is observed with AdoMet, a V-type allosteric effector, which enhances  $k_{\text{cat}}$  ~2-fold (8) and is presumed to bind to the regulatory domain (11).

Mutations in cystathionine  $\beta$ -synthase are the single most common cause of homocystinuria and over 100 disease-associated mutations have been identified in patients (12). A subset of these pathogenic mutations maps to the regulatory domain appears to impose a conformational lock on the protein and is unresponsive to AdoMet (13, 14). While the structure of the N-terminal catalytic core of cystathionine  $\beta$ -synthase has been determined (5, 6), no structural information is available for the regulatory domain, where the allosteric activator is presumed to bind (11). In this study, we have employed hydrogen exchange mass spectrometry (MS) to identify peptides that respond to the presence of AdoMet and those that respond to deletion of the regulatory domain, to locate regions associated with intrasteric inhibition and allosteric activation, respectively.

## EXPERIMENTAL SECTION

**Materials.** Deuterium oxide (100.00 atom % D) was purchased from Sigma. Pepsin (from porcine stomach mucosa), and protease inhibitors were purchased from Sigma, porcine trypsin was from Promega and thrombin (bovine) was purchased from GenTrac Inc. Middleton, WI.

**Enzyme Purification.** Wild-type enzyme, the C-terminal truncated form (designated  $\Delta$ C143), and the D444N mutant were expressed and purified as previously described (8, 14, 15).

**Limited Proteolysis of Cystathionine  $\beta$ -Synthase.** Cystathionine  $\beta$ -synthase was subjected to limited proteolysis

<sup>†</sup> This work was supported in part by a grant from the National Institutes of Health (HL58984 and P20RR17675).

\* Corresponding author. Tel: (402)-472-2941, e-mail: rbanerjee1@unl.edu.

<sup>1</sup> Abbreviations: AdoMet, S-adenosylmethionine; MS, mass spectrometry; ESI, electrospray ionization.

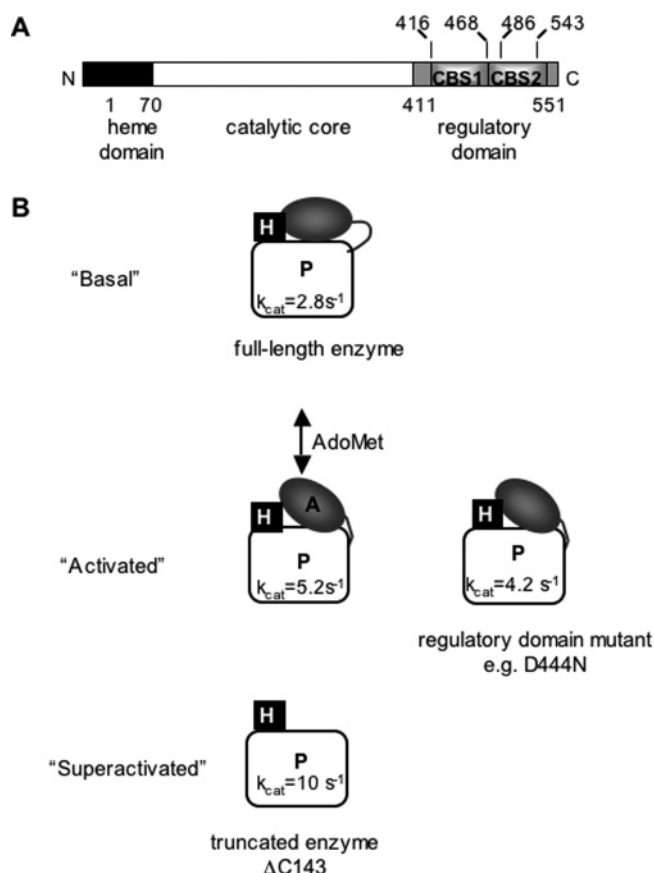


FIGURE 1: Modular organization and kinetic forms of human cystathionine  $\beta$ -synthase. A. The domains in human cystathionine  $\beta$ -synthase include an N-terminal heme domain, a central catalytic core and a C-terminal regulatory domain containing a tandem repeat of two CBS domains. B. Kinetically distinguishable states of human cystathionine  $\beta$ -synthase. A, P, and H denote AdoMet, PLP, and heme, respectively.

as described in the Figure 2 caption and quenched at the desired times with  $N^\alpha$ -*p*-tosyl-L-lysine chloromethyl ketone (Sigma).

**Hydrogen–Deuterium Exchange.** The feasibility of the H/D exchange MS method was initially assessed for cystathionine  $\beta$ -synthase by determining the sequence coverage and the spectral quality of its peptides. For this, cystathionine  $\beta$ -synthase (10  $\mu$ g) in 100 mM ammonium phosphate buffer, pH 2.2, was centrifuged to remove any insoluble matter and digested with pepsin (1:1 w/w) for 5 min on ice. The peptic fragments were separated by HPLC and identified by tandem ESI-MS/MS as described below. Approximately 76% sequence coverage was obtained (Table 1 and Figure 2). One of the major peptides that was not observed in this analysis extends from residues 252–287 and resides in a protease resistant core of the protein (16). Additionally, the peptides in the N-terminal heme domain were not detected, which could have resulted from a paucity of pepsin cleavage sites in this region.

The mutant enzymes,  $\Delta$ C143 and D444N (10  $\mu$ g and 20  $\mu$ g respectively) in 10 mM phosphate buffer, pH 6.8, were diluted 20-fold in the exchange buffer prepared in D<sub>2</sub>O (10 mM phosphate buffer, pD 6.8). For samples containing cystathionine  $\beta$ -synthase complexed with AdoMet, the enzyme was preincubated with 1 mM AdoMet at room temperature for 2 h. For H/D exchange studies, samples were

Table 1: Cystathionine  $\beta$ -Synthase Peptides Detected by Mass Spectrometry

no.	peptide boundary	sequence
1	73–81	SPKILRDIL
2	106–111	LAKCEF
3	112–124	FNAGGSVKDRISL
4	125–153	RMIEDAERDGTLPKPGDTTHIEPTSGNTGIG
7	127–156	IEDAERDGTLPKPGDTTHIEPTSGNTGIGLAL
8	154–165	LALAAAVRGYRC
9	155–165	ALAAAVRGYRC
10	166–176	IIVMPEKMSSE
11	166–181	IIVMPEKMSSEKVDVL
12	166–187	IIVMPEKMSSEKVDVLRALGAE
13	177–181	KVDVL
14	177–187	KVDVLRALGAE
15	188–197	IVRTPTNARF
16	198–222	DSPESHVGVAVRLKNEIPNSHILDQ
17	223–238	YRNASNPLAHYDTTAD
18	223–239	YRNASNPLAHYDTTADAE
19	223–241	YRNASNPLAHYDTTADAIL
20	240–248	ILQQCDGKL
21	242–251	QQCDGKLDML
22	288–302	AEPEELNQTEQTTYE
23	303–315	VEGIGYDFIPTVL
24	316–323	DRTVVDKW
25	316–331	DRTVVDKWFKSNDEEA
26	316–333	DRTVVDKWFKSNDEEAFT
27	325–334	KSNDEEAFTF
28	338–355	LIAQEGLLCGGSAGSTVA
29	356–370	VAVKAAQELQEGQRC
30	371–385	VVILPDSVRNYMTKF
31	386–397	LSDRWMLQKGFL
32	386–401	LSDRWMLQKGFLKEED
33	391–397	MLQKGFL
34	398–412	KEEDLTEKKPWVWHL
35	413–426	RVQELGLSAPLTVL
36	415–426	QELGLSAPLTVL
37	417–426	LGLSAPLTVL
38	427–438	PTTCGHTIEL
39	437–453	ILREKGFQAPVVDEAG
40	437–457	ILREKGFQAPVVDEAGVILG
41	437–458	ILREKGFQAPVVDEAGVILGM
42	439–453	REKGFQAPVVDEAG
43	439–458	REKGFQAPVVDEAGVILGM
44	459–464	VTLGNM
45	459–468	VTLGNMSSL
46	465–469	LSSLL
47	469–492	LAGKVQPSDQVGKVIYKQFKQIRL
48	493–510	TDTLGRSLSHILEMDHFAL
49	505–510	MDHFAL
50	511–531	VVHEQIQYHSTGKSSQRQMV
51	532–536	GVVTA
52	536–539	AIDL
53	536–541	AIDLLN
54	536–542	AIDLLNF
55	542–551	FVAAQERDQK

incubated at room temperature for 5 to 60 s (to determine the effect of AdoMet) or between 5 s and 21 h (to monitor the kinetics of hydrogen exchange in full-length enzyme and the truncated variant,  $\Delta$ C143) and quenched by a 2-fold dilution with 100 mM ammonium phosphate buffer, pH 2.2. The quenched samples were immediately frozen in liquid nitrogen and stored at  $-80^\circ\text{C}$  until further use. Following thawing, the samples were digested with pepsin as described above.

To correct for loss of deuterium incurred under the experimental conditions, the peptide mass was determined using eq 1

$$D = \frac{(m - m_{0\%})}{(m_{100\%} - m_{0\%})} XN \quad (1)$$

where  $D$  is the adjusted deuterium incorporation,  $m$  is the

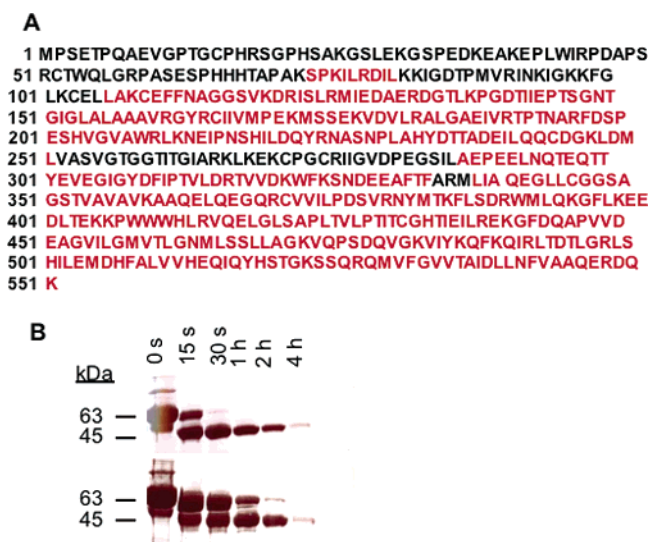


FIGURE 2: A. Sequence coverage of human cystathionine  $\beta$ -synthase obtained by MS analysis is shown in red. B. Limited proteolysis of human cystathionine  $\beta$ -synthase. Cystathionine  $\beta$ -synthase (5 nmol) was incubated at 37 °C with 750 units of porcine trypsin in 50 mM ammonium bicarbonate buffer, pH 8, in the absence (upper) or presence of 32  $\mu$ M AdoMet (lower) for 0 s, 15 s, 30 s, 1 h, 2 h, and 4 h, respectively. The reaction was quenched with 1 mM TLCK. The peptide mixture was resolved by 10% SDS PAGE and visualized by Coomassie blue staining.

experimentally observed mass at a given time,  $m_{0\%}$  is the 0% or undeuterated control,  $m_{100\%}$  is the fully deuterated control, and  $N$  is the total number of exchangeable amide protons (and excludes the N-terminal proton and any proline residues). To obtain the  $m_{0\%}$  value, 20  $\mu$ g of protein was diluted 20-fold in the quench buffer followed rapidly by the addition of an equal amount of exchange buffer in  $D_2O$  and digested with pepsin as described above. Thus, the final composition of deuterium in the quench and dilution solutions was identical for the samples and the corresponding  $m_{0\%}$  control.

To obtain the  $m_{100\%}$  value, a fully deuterated sample was prepared by incubating 20  $\mu$ g of the protein overnight at room temperature in an 8 M guanidinium hydrochloride solution prepared in  $D_2O$ . The protein sample was subsequently diluted 10-fold with 100 mM ammonium phosphate, pH 2.2 (at which concentration the denaturant does not interfere with proteolytic digestion), prior to pepsin treatment. On average, ~25% of the deuterium was lost due to back exchange.

**HPLC-ESI Mass Spectrometry.** LC/ESI-MS was employed to determine the extent of deuterium incorporation into individual peptides. The HPLC injection loop, chromatographic buffers, and all the tubing used in the LC-MS set up were submerged in ice to minimize deuterium loss in this step. The peptic peptides were separated by reversed phase HPLC using a microbore C18 column (5 cm length  $\times$  1 mm internal diameter, Micro-Tech Scientific, Cousteau Court, CA). The solvents used for separation were A (water, 0.3% formic acid) and B (acetonitrile, 0.3% formic acid). The gradient was 10–35% solvent B over 20 min at a flow rate of 40  $\mu$ l/min. Peptides were initially identified by tandem ESI-MS/MS sequencing. The masses of individual peptides in hydrogen exchange experiments were determined by ESI-MS on a Quadrupole Time-of-Flight mass spectrometer (Applied Biosystems). The peak for each peptide was integrated to obtain a centroid value using the Magtran

computer program (17). The deuterium incorporation for each peptide was quantified by calculating the difference between the centroid values before and after deuterium exchange at a given time point using eq 1.

**Modeled Structures.** A model for the regulatory domain of human cystathionine  $\beta$ -synthase extending from residues 411–551 was calculated using SWISS-MODEL (18) using the 120 amino acid long CBS domain-containing protein from *Methanothermobacter thermautotrophicus* (Archae), strain delta H (PDB-ID 1PBJ).

A docking model for the interaction between the known structure of the dimeric catalytic core (1M54) and the modeled structure of one regulatory domain was generated using ZDOCK, which combines pairwise shape complementarity with desolvation and electrostatics for scoring unbounded docking models (19). The search returned 3600 docking positions, with scores ranging from 62.29 to 30.09. To generate a model of the full-length dimer, the single regulatory domain obtained from the docked model was rotated around the noncrystallographic C2 symmetry axis of the A and B chains of the catalytic domain.

To narrow down the number of docked candidates, the following filter was applied: that the C $\alpha$  of one of the exposed residues in the 356–370 peptide in the catalytic domain (358, 359, 362, 363, 365, 366 or 369) is within 4.5–6 Å of any C $\alpha$  in the regulatory domain. Of the top thirty hits on the score chart, only five satisfied this criterion and the remaining models were excluded. The five candidates fell into two groups with the top two and bottom three models being very similar with respect to their overall disposition of the catalytic and regulatory domains. The bottom three models placed the regulatory domains at two ends of the dimer, making it difficult to envision them as surfaces for tetramerization. Of the two top candidates (with the 2nd and 6th highest scores in the original list of 3600 hits), one (# 6) was selected for further analysis because it afforded more favorable interactions between the dimers at the presumed dimer–dimer interface. In this model, the distance between the last structured residue in the C-terminus of the catalytic domain (C $\alpha$  of K395) and the first structured residue in the N-terminus of the regulatory domain (C $\alpha$  of Q414) is 49.1 Å, a distance that can potentially be connected by the 20 intervening amino acids.

## RESULTS AND DISCUSSION

Cystathionine  $\beta$ -synthase is poised at a critical metabolic junction where the decision to conserve homocysteine in the methionine cycle or to commit it to transsulfuration is made. It is therefore not surprising that the enzyme is subjected to complex regulation, which includes intrasteric inhibition imposed by the C-terminal domain and allosteric activation induced by AdoMet (4). Curiously, a subset of pathogenic cystathionine  $\beta$ -synthase mutations have been described that map to the regulatory domain, display a higher level of basal activity, but are unresponsive to AdoMet (13, 14). This apparently paradoxical phenotype associated with pathogenic mutations is enigmatic and begs the question as to why they are correlated with disease.

Structural insight into these regulatory modes is limited by the availability of the crystal structure of only the truncated, dimeric form of the enzyme lacking the regulatory



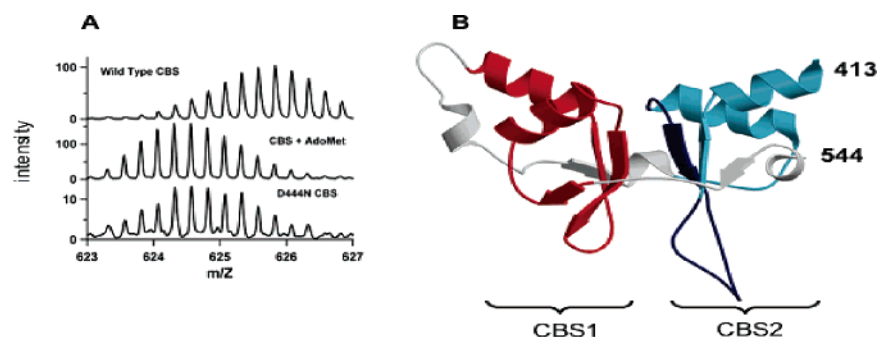


FIGURE 3: Mapping allosteric effects. A. Comparison of the mass analysis of the 511–531 peptide after 30 s of hydrogen exchange in wild-type enzyme without (upper) and with (middle) AdoMet and in the D444N mutant lacking AdoMet (lower). B. Location of the 513–531 peptide (in navy) in the modeled structure of the C-terminal domain. The CBS1 and CBS2 domains are shown in red and blue, respectively, and the model extends from residues 413–544 of cystathionine  $\beta$ -synthase.

domain. Hence, the relative juxtaposition of the regulatory and catalytic domains and the location of the dimer–dimer interface in the full-length enzyme are unknown. Kinetic studies indicate that the wild-type enzyme equilibrates between at least two conformations, the “basal” state and the “activated state”, which is induced by AdoMet (Figure 1) (14). Limited proteolysis of wild-type cystathionine  $\beta$ -synthase in the presence and absence of AdoMet reveals differences in the kinetics of degradation of the protein (Figure 2), consistent with a conformational alteration. Thus, AdoMet stabilizes cleavage of the enzyme at the hypersensitive site between the catalytic and regulatory domains that converts the full-length 63 kDa subunit to a truncated 45 kDa one.

The pathogenic D444N mutant exhibits a  $k_{\text{cat}}$  that is similar to the “activated” state of wild-type enzyme, albeit in the absence of AdoMet, while the truncated dimer exists in a “superactivated” state, with a  $k_{\text{cat}}$  that is  $\sim 4$ -fold higher than that of the “basal” state (Figure 1). The D444N mutation increases the  $K_d$  for AdoMet binding to the regulatory domain from  $34 \pm 2 \mu\text{M}$  to  $510 \pm 70 \mu\text{M}$  consistent with the observed insensitivity of the mutant to physiological concentrations of the allosteric effector (11). Hydrogen exchange MS was employed to assess whether these discrete kinetic states could be correlated to conformational ones and to localize peptides that are sensitive to binding of AdoMet and to deletion of the regulatory domain.

**AdoMet-Induced Changes in Hydrogen Exchange Kinetics.** The effect of AdoMet on the extent of deuterium incorporation was monitored over a 5 to 60 s time range. Analysis of the mass distribution profiles of  $> 50$  peptides revealed a very focal conformational difference. The uncertainty in our mass measurements is  $\sim 0.2$ – $0.3$  deuteriums, and the difference in deuterium incorporation in all but one of the peptides from the two forms of the cystathionine  $\beta$ -synthase, fell within this range. Only a single peptide extending from residues 511–531 was identified that was sensitive to the presence of AdoMet (Figure 3B). A significant shift in the average mass from 2503.36 (–AdoMet) to 2498.24 (+AdoMet) was observed for this peptide indicative of either lower solvent accessibility or reduced hydrogen bonding in the presence of AdoMet. This represents a decrease in deuterium incorporation, from 85.5% to 51.6%, relative to the maximum deuterium incorporation possible for this peptide.

The observed binomial distribution of isotope peaks for this peptide, which is characteristic of EX2 or “uncorrelated exchange” indicates that a high level of structural homogeneity exists during the deuterium exchange-in time (20). In

other words, the unimodal distribution of the peptide mass envelope in the presence or absence of AdoMet indicates that under the present experimental conditions, the enzyme is seen to populate either the “basal” or the “activated” state and an equilibrium mixture between these two states is not detected. This is in contrast to the hematopoietic cell kinase SH3 domain in which interconverting conformers are detected by hydrogen exchange MS (21).

Two limitations of the hydrogen exchange MS approach that are also pertinent to this study bear note. First, differences in deuterium exchange kinetics of peptides that occur on a fast time scale ( $< 5$  s) would have been missed in this study. Second, although the 76% coverage of amino acids obtained in this experiment is relatively high, differences in the remaining 24% of the protein are missed. Approximately half of the missing residues that we were unable to detect reside in a protease resistant region of the protein, as discussed under Methods, with most of the remainder being in the N-terminal heme domain.

**The D444N Mutant is Conformationally Locked in the “Activated” State.** Since the pathogenic D444N mutant is unresponsive to physiological concentrations of AdoMet (14), the mutation could in principle have locked the protein in either the “basal” or the “activated” conformation. To distinguish between these two possibilities, the kinetics of hydrogen exchange for the D444N mutant were compared to that of wild-type enzyme. They were found to be virtually identical to that of wild-type enzyme in the presence of AdoMet (Figure 3B). Thus, the D444N is locked in the “activated” conformation in the absence of AdoMet binding, which is consistent with its high basal activity and its insensitivity to physiological concentrations of AdoMet (Figure 3).

**Modeled Structure of the C-Terminal Regulatory Domain.** Conformational perturbation of the 511–531 peptide is particularly interesting since it is located in the C-terminal module of the enzyme (Figure 1) where AdoMet is predicted to bind (11). This module harbors a tandem repeat of two CBS domains, a secondary structure motif that is predicted to adopt a  $\beta$ – $\alpha$ – $\beta$ – $\beta$ – $\alpha$  fold and is found in diverse proteins in all three kingdoms of life (22). This domain, which derives its name from its presence in cystathionine  $\beta$ -synthase, is believed to function as an energy-sensing module and typically binds nucleotides (11). Since the structure of the full-length cystathionine  $\beta$ -synthase is unavailable, we have generated a homology modeled structure of the C-terminal regulatory domain (Figure 3C) using

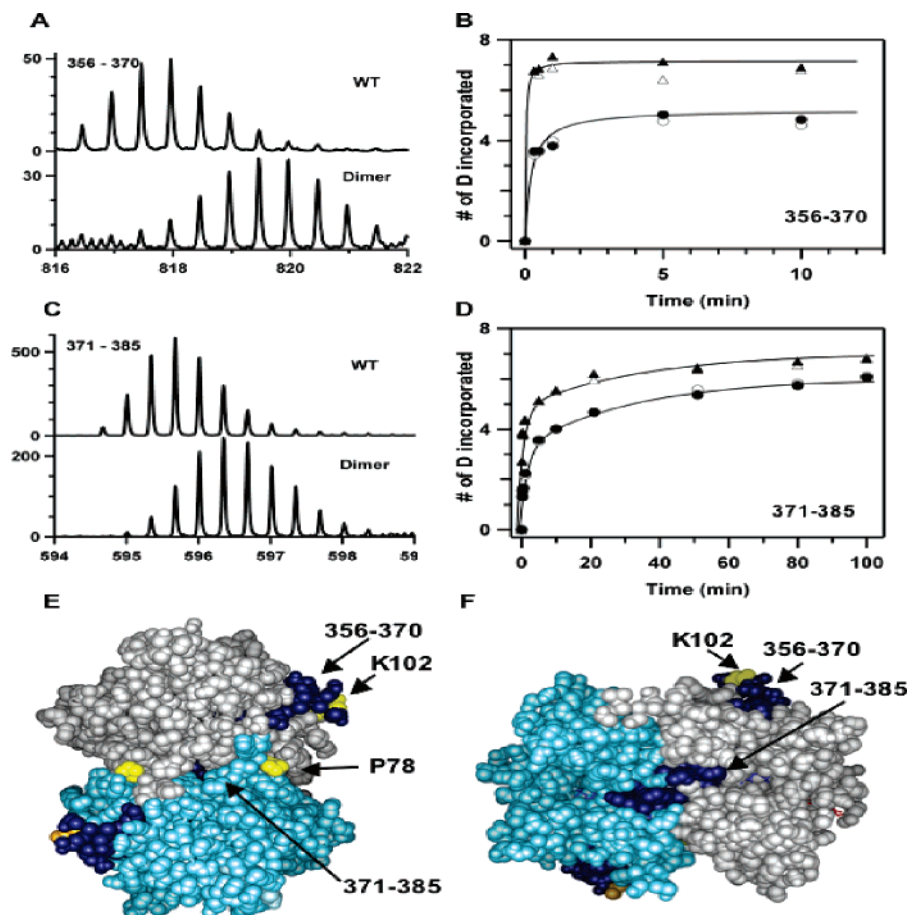


FIGURE 4: Mapping intrasteric effects. A. Comparison of the kinetics of hydrogen exchange of peptides 356–370 (A) and 371–385 (B) that respond to deletion of the regulatory domain. The spectra in A and B represent samples that were quenched after 1 min. C and D show the differences in the kinetics of deuterium incorporation in the 356–370 peptide in the truncated (circles) and full-length (triangles) protein (C) and for the 371–385 peptide in truncated (circles) and full length (triangles) protein (D). The closed and open symbols represent data from two independent experiments. E. Location of the 356–370 and 371–385 peptides (in navy) in the crystal structure of the catalytic core shown in surface representation. The subunits are shown in gray and blue, and the residues, P78 and K102, that are mutated in some homocystinuric patients and lead to lack of AdoMet sensitivity are shown in yellow. F. A different view of the truncated dimer highlighting the location of the 371–385 peptide.

the coordinates for a CBS domain protein from *M. thermoautotrophicus*.

Pairs of CBS domains are known to dimerize to form a stable globular domain, which is also the case in the modeled structure for the cystathionine  $\beta$ -synthase C-terminal domain. The 511–531 peptide resides in the CBS2 domain and exhibits sensitivity to AdoMet binding and also to the D444N mutation in the CBS1 domain. The sensitivity of the 511–531 peptide could be a consequence of its proximity to the binding site for AdoMet and/or its location on the pathway of allosteric signal transduction, a distinction that cannot be made by the hydrogen exchange MS approach.

**Identification of Peptides That Respond to Deletion of the Regulatory Domain.** C-Terminal truncation leads to a change in the oligomerization state from  $\alpha_4$  to  $\alpha_2$  and generates a “superactivated” form of the enzyme (Figure 1). This form is observed physiologically in response to a proinflammatory challenge induced by TNF $\alpha$  or lipopolysaccharide and increases the flux of homocysteine through cystathionine  $\beta$ -synthase, leading eventually to increased synthesis of the antioxidant, glutathione (10).

Surprisingly, deletion of the regulatory domain leads to very focal changes in the kinetics of deuterium exchange

within the time frame of our observations, which extended from 5 s to 21 h. Only two peptides, contiguous in sequence space, displayed significant differences in deuterium incorporation (Figure 4A–D). The first peptide extends from residues 356–370 (Figure 4E). Several amino acids in this segment are quite surface-exposed, particularly residues 358, 359, 362, 363, 365, 366, and 369. It is interesting to note that several pathogenic mutations have been reported in this stretch of cystathionine  $\beta$ -synthase including one, R369C/H, which is surface exposed in the dimeric structure (12). A maximum difference in deuterium incorporation in this peptide was seen after a 1 min exposure to D<sub>2</sub>O (Figure 4B). The centroid mass shifted from 1635.234 (full-length) to 1636.528 in the truncated enzyme, which represents a change from 25% to 41% of maximal deuterium incorporation seen for this peptide.

The second peptide, extending from residues 371–385, is largely buried and resides at the interface between the monomers (Figure 4F). Only residues 382–384 in this peptide are surface-exposed and are located at the base of a cavern. A maximum mass difference in this peptide is observed after 10 min of exposure to D<sub>2</sub>O (Figure 4D). The centroid mass shifted from an average of 1788.969 (full-length) to 1791.342 (truncated), which represents an increase

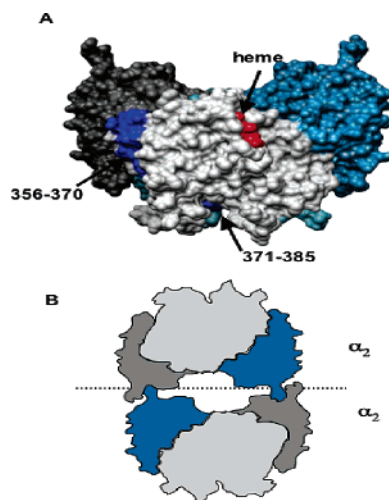


FIGURE 5: Modeled structure of full-length cystathionine  $\beta$ -synthase. A. A docked model showing the predicted juxtaposition of the regulatory domains and the catalytic core of the dimer. The two catalytic domains are shown in light gray and light blue, respectively, while the corresponding regulatory domains are shown in darker shades. The light blue subunit is behind the plane of the light gray subunit and not visible. A portion of the 356–370 peptide (in navy) on one of the chains and of the heme (in red) are visible in this view. This model was generated using ZDOCK as described under Methods. B. Model of the full-length cystathionine  $\beta$ -synthase showing the relative juxtaposition of two  $\alpha_2$  dimers. The color scheme used in A is retained.

from 25% to 52.1% of the maximal deuterium incorporation seen for this peptide. Several patient mutations have been identified in this stretch of cystathionine  $\beta$ -synthase, including one, K384N/E that is exposed in the dimeric structure (12).

**A Modeled Structure for Full-Length Cystathionine  $\beta$ -Synthase.** The hydrogen exchange data identifies two surfaces in the dimeric structure that experience greater solvent accessibility or reduced hydrogen bonding interactions upon deletion of the regulatory domain (Figure 4E and 4F). We have employed the MS data in conjunction with the reported properties of cystathionine  $\beta$ -synthase to guide our selection of a model for the full-length enzyme (Figure 5) generated by the ZDOCK program.

It is important, however, to first note some limitations of this model-building exercise. In principle, it is possible that the peptides identified in this study report indirectly on the loss of the regulatory domain with a consequent change in the oligomeric organization, and that the actual interaction surfaces were missed due to the time course of the kinetic analysis. Hydrogen exchange rates for individual amides in a protein can vary over several orders of magnitude (23), and only those amides with half-lives for exchange that are similar to the experimental labeling time report on structural changes (20). Thus, a limitation of this study is that hydrogen exchange kinetics were monitored in a time range from seconds to hours, and differences in dynamics and/or structure that resulted in differences in deuterium incorporation rates on a shorter time scale would have been missed.

We propose that both the 356–370 and the 371–385 peptides are likely to be reporting on deletion of the regulatory domain based on the following lines of reasoning. Cystathionine  $\beta$ -synthase exists as a homotetramer that separates into dimers following a proteolytic clip between

the catalytic and regulatory domains (16). Thus, interactions between the regulatory domains appear to be more important in preserving the tetrameric structure than interactions between the catalytic domains. We propose that the 356–370 peptide is involved in making direct contact with the regulatory domain based on its proximity to the P78 and K102 residues (Figure 4E). Mutations in these two residues (P78R/K102N) are inherited as linked pathogenic mutations in homocystinurics (12). The P78R/K102N mutations impair sensitivity to AdoMet, suggesting their proximity to the regulatory domain (Sen and Banerjee, manuscript in preparation). The docked model generated by ZDOCK provides an excellent fit to our assignment of this region as the regulatory–catalytic domain interface (Figure 5 A).

The exposed surface of the 371–385 peptide is located at the bottom of a cavity (Figure 5A) and leads to a short helix that ends in a loop representing the C-terminus of the catalytic domain. In the intact structure, this loop would lead to the regulatory domain and its truncation could perturb the environment of the 371–385 peptide, resulting in changes in the kinetics of deuterium incorporation. The location and the limited surface exposure of this largely buried peptide appear to be incompatible with its possible involvement in the dimer–dimer interface (Figure 5).

Based on the docked model of the dimer, we propose a schematic model for the organization of the full-length enzyme (Figure 5B). In this model, the regulatory domains on adjacent monomers are on opposite edges of the dimer and contact the mirror domains in the tetramer. This model is consistent with the known properties of the wild type and mutant enzymes, the role of the regulatory domain in tetramerization, and with the separation of dimers following deletion of this domain. In this model, the regulatory domains form the dimer–dimer interface and generation of the truncated dimer exposes on the catalytic domain only those surfaces that are sensitive to loss of the regulatory domain. This is consistent with our ascription of the sensitivity of both the 356–370 and 371–385 peptides to deletion of the regulatory domain. The validity of this model will of course be tested as additional insights into cystathionine  $\beta$ -synthase are gained and ultimately by the crystal structure of the full-length enzyme itself.

## CONCLUSIONS

In summary, we have localized focal conformational changes in wild-type cystathionine  $\beta$ -synthase that are induced by AdoMet, to a peptide which spans residues 511–531 in the regulatory domain. Furthermore, we have demonstrated that this “activated” conformation is mimicked by the pathogenic D444N mutation, explaining its known insensitivity to AdoMet (14, 24). This approach could be useful for providing structural insights into other pathogenic mutants. The kinetics of hydrogen exchange reveal two surfaces that are sensitive to deletion of the regulatory domain. This information has been used to build a structural model of the full-length human enzyme (Figure 5), which could be helpful in providing a framework for understanding the interactions between the regulatory and catalytic modules and the penalties associated with pathogenic mutants.



## ACKNOWLEDGMENT

The authors thank David Smith (University of Nebraska, Lincoln) for his helpful comments on the manuscript. The Mass Spectrometry Core Facility of the Redox Biology Center (University of Nebraska, Lincoln) was used in this study and supported by a grant from the NIH (P20RR17675).

## REFERENCES

1. Hoofnagle, A. N., Resing, K. A., and Ahn, N. G. (2003) Protein analysis by hydrogen exchange mass spectrometry, *Annu. Rev. Biophys. Biomol. Struct.* 32, 1–25.
2. Engen, J. R., and Smith, D. L. (2000) Investigating the higher order structure of proteins. Hydrogen exchange, proteolytic fragmentation, and mass spectrometry, *Methods Mol. Biol.* 146, 95–112.
3. Miles, E. W., and Kraus, J. P. (2004) Cystathionine {beta}-Synthase: Structure, Function, Regulation, and Location of Homocystinuria-causing Mutations, *J. Biol. Chem.* 279, 29871–29874.
4. Banerjee, R., and Zou, C. G. (2005) Redox regulation and reaction mechanism of human cystathionine-beta-synthase: a PLP-dependent hemesensor protein, *Arch. Biochem. Biophys.* 433, 144–156.
5. Meier, M., Janosik, M., Kery, V., Kraus, J. P., and Burkhard, P. (2001) Structure of human cystathionine beta-synthase: a unique pyridoxal 5'-phosphate-dependent heme protein, *EMBO J.* 20, 3910–6.
6. Taoka, S., Lepore, B. W., Kabil, Ö., Ojha, S., Ringe, D., and Banerjee, R. (2002) Human cystathionine beta-synthase is a heme sensor protein. Evidence that the redox sensor is heme and not the vicinal cysteines in the CXXC motif seen in the crystal structure of the truncated enzyme, *Biochemistry* 41, 10454–61.
7. Kery, V., Bukovska, G., and Kraus, J. P. (1994) Transsulfuration depends on heme in addition to pyridoxal 5'-phosphate. Cystathionine  $\beta$ -synthase is a heme protein, *J. Biol. Chem.* 269, 25283–25288.
8. Taoka, S., Widjaja, L., and Banerjee, R. (1999) Assignment of enzymatic functions to specific regions of the PLP-dependent heme protein cystathionine  $\beta$ -synthase, *Biochemistry* 38, 13155–13161.
9. Shan, X., and Kruger, W. D. (1998) Correction of disease causing CBS mutations in yeast, *Nature Genet.* 19, 91–93.
10. Zou, C.-G., and Banerjee, R. (2003) Tumor necrosis factor- $\alpha$ -induced targeted proteolysis of cystathionine beta-synthase modulates redox homeostasis, *J. Biol. Chem.* 278, 16802–16808.
11. Scott, J. W., Hawley, S. A., Green, K. A., Anis, M., Stewart, G., Scullion, G. A., Norman, D. G., and Hardie, D. G. (2004) CBS domains form energy-sensing modules whose binding of adenosine ligands is disrupted by disease mutations, *J. Clin. Invest.* 113, 274–84.
12. Kraus, J. P., Janosik, M., Kozich, V., Mandell, R., Shih, V., Sperandio, M. P., Sebastio, G., de Franchis, R., Andria, G., Kluijtmans, L. A., Blom, H., Boers, G. H., Gordon, R. B., Kamoun, P., Tsai, M. Y., Kruger, W. D., Koch, H. G., Ohura, T., and Gaustadnes, M. (1999) Cystathionine beta-synthase mutations in homocystinuria, *Hum. Mutat.* 13, 362–75.
13. Janosik, M., Kery, V., Gaustadnes, M., Maclean, K. N., and Kraus, J. P. (2001) Regulation of human cystathionine beta-synthase by S-adenosyl-L-methionine: evidence for two catalytically active conformations involving an autoinhibitory domain in the C-terminal region, *Biochemistry* 40, 10625–33.
14. Evande, R., Boers, G. H. J., Blom, H. J., and Banerjee, R. (2002) Alleviation of Intrasteric Inhibition by the Pathogenic Activation Domain Mutation, D444N, in Human Cystathionine beta-synthase, *Biochemistry* 41, 11832–11837.
15. Taoka, S., Ohja, S., Shan, X., Kruger, W. D., and Banerjee, R. (1998) Evidence for heme-mediated redox regulation of human cystathionine  $\beta$ -synthase activity, *J. Biol. Chem.* 273, 25179–25184.
16. Kery, V., Poneleit, L., and Kraus, J. (1998) Trypsin cleavage of human cystathionine beta-synthase into an evolutionarily conserved active core: Structural and functional consequences, *Arch. Biochem. Biophys.* 355, 222–232.
17. Zhang, Z., and Smith, D. L. (1993) Determination of amide hydrogen exchange by mass spectrometry: a new tool for protein structure elucidation, *Protein Sci.* 2, 522–31.
18. Schwede, T., Kopp, J., Guex, N., and Peitsch, M. C. (2003) SWISS-MODEL: An automated protein homology-modeling server, *Nucleic Acids Res.* 31, 3381–5.
19. Chen, R., Li, L., and Weng, Z. (2003) ZDOCK: an initial-stage protein-docking algorithm, *Proteins* 52, 80–7.
20. Smith, D. L. (1998) Local structure and dynamics in proteins characterized by hydrogen exchange and mass spectrometry, *Biochemistry (Mosc)* 63, 285–93.
21. Engen, J. R., Smithgall, T. E., Gmeiner, W. H., and Smith, D. L. (1997) Identification and localization of slow, natural, cooperative unfolding in the hematopoietic cell kinase SH3 domain by amide hydrogen exchange and mass spectrometry, *Biochemistry* 36, 14384–91.
22. Bateman, A. (1997) The structure of a domain common to archaeobacteria and the homocystinuria disease protein., *Trends Biochem. Sci.* 22, 12–13.
23. Englander, S. W., Downer, N. W., and Teitelbaum, H. (1972) Hydrogen exchange, *Annu. Rev. Biochem.* 41, 903–24.
24. Kluijtmans, L. A. J., Boers, G. H. J., Stevens, E. M. B., Renie, W. O., Kraus, J. P., Trijbels, F. J. M., Heuvel, L. P. W. J. v. d., and Blom, H. J. (1996) Defective cystathionine beta-synthase regulation by S-adenosylmethionine in a partially pyridoxine responsive homocystinuria, *J. Clin. Invest.* 98, 285–289.

BI051046D